

# Single Top Quark at Future Hadron Colliders. Complete Signal and Background Study.

A. S. Belyaev<sup>1,2</sup>, E. E. Boos<sup>2</sup>, L. V. Dudko<sup>2</sup>

<sup>1</sup> *Instituto de Física Teórica, Universidade Estadual Paulista,  
Rua Pamplona 145, 01405-900 São Paulo, Brazil.*

<sup>2</sup> *Skobeltsyn Institute of Nuclear Physics, Moscow State University  
119899 Moscow, Russian Federation*

We perform a detail theoretical study including decays and jet fragmentation of all the important modes of the single top quark production and all basic background processes at the upgraded Tevatron and LHC colliders. Special attention was paid to the complete tree level calculation of the QCD fake background which was not considered in the previous studies. Analysis of the various kinematical distributions for the signal and backgrounds allowed to work out a set of cuts for an efficient background suppression and extraction of the signal. It was shown that the signal to background ratio after optimized cuts could reach about 0.4 at the Tevatron and 1 at the LHC. The remaining after cuts rate of the signal at the LHC for the *lepton + jets* signature is expected to be about 6.1 pb and will be enough to study the single top physics even during the LHC operation at a low luminosity.

## I. INTRODUCTION

The existence of the top quark has been established in March 1995 by the CDF and DØ collaborations at the Tevatron collider. [1]. Top quark has been discovered in the strong  $t\bar{t}$  pair production mode.

The cross section of electroweak process of single top quark was found to be comparable with the QCD pair top production [2]. Single top production mechanism is the independent way of a confirmation of the top quark existence and straightforward key to measure the  $Vtb$  CKM matrix element and to study the  $Wtb$  vertex. Since the mass of the top quark is very large compared to all other quarks one might expect some deviations from the Standard Model (SM) predictions in the top quark interactions [3]. The single top quark production rate is directly proportional to the  $Wtb$  coupling and therefore it is a promising place to look for deviations from the SM.

However one should stress that the task of background reduction is much more serious and important problem in the case of the single top comparing to the  $t\bar{t}$ -pair production. It happens because the jet multiplicity of single top quark events is typically less than for  $t\bar{t}$ -pair production and so QCD  $Wjj$  and multijet backgrounds are much higher, and the problem of the single top signal extraction is more involved. That is why the detail background study is especially needed in order to find an optimal strategy to search for of single top quark.

Top quark decays into a  $W$ -boson and a  $b$  quark with the almost 100% branching ratio in the framework of the Standard Model. We consider here the subsequent leptonic decays of the  $W$ -boson to a electron (muon) and neutrino, as this signal has much less background and should be easier to find experimentally than channels with hadronic decay of the  $W$  boson.

## II. MC SIMULATION

In order to study a possibility of the signal extraction from the background we have created the MC generator for complete set of the single top production and backgrounds processes. Generator was designed as a new external user process for the PYTHIA 5.7/JETSET 7.4 package [4]. This generator is related to PYTHIA 5.7 by a special interface and uses FORTRAN codes of squared matrix elements produced by the package CompHEP [5]. For integration over the phase space and a consequent event simulation the Monte-Carlo generator uses the kinematics with a proper smoothing of singular variables [6] from the CompHEP and the integrator package BASES/SPRING [7].

The effects of the final state radiation, hadronization and string jet fragmentation (by means of JETSET 7.4) have also been taken into account. The following resolutions have been used for the jet and electron energy smearing:  $\Delta E^{had}/E = 0.5/\sqrt{E}$  and  $\Delta E^{ele}/E = 0.2/\sqrt{E}$ . In our analysis we used the cone algorithm for the jet reconstruction with the cone size  $\Delta R = \sqrt{\Delta\varphi^2 + \Delta\eta^2} = 0.5$ . The minimum  $E_T$  threshold for a cell to be considered as a jet initiator has been chosen 5 GeV while the one of summed  $E_T$  for a collection of cells to be accepted as a jet has been chosen 10 GeV.

For all calculations CTEQ3M parton distribution has been used. For the top-quark production we chose the QCD  $Q^2$  scale equal to the top mass squared, while for  $Wjj$  background  $Q^2 = M_W^2$  have been taken. For calculations of  $jb\bar{b}$  and  $jjb\bar{b}$  processes we chose the invariant  $b\bar{b}$  mass for the  $Q^2$  scale.

Under the assumptions mentioned above the kinematic features of both signatures for signal and background have been studied.

### A. Signal

We concentrated on the following set of processes at Tevatron  $p\bar{p}$  and LHC  $pp$  colliders leading to the single top quark production:

1.  $p\bar{p} \rightarrow tqb\bar{b} + X$ ,
2.  $p\bar{p} \rightarrow t\bar{b}b + X$ ,
3.  $p\bar{p} \rightarrow tq + X$ ,
4.  $p\bar{p} \rightarrow tW + X$ ,

where  $q$  is a light quark and  $X$  represents the remnants of the proton and antiproton. Basic Feynman diagrams for processes mentioned above are shown in Fig. 1. We refer to the paper [8] which consider the whole set of Feynman diagrams for signal subprocesses.

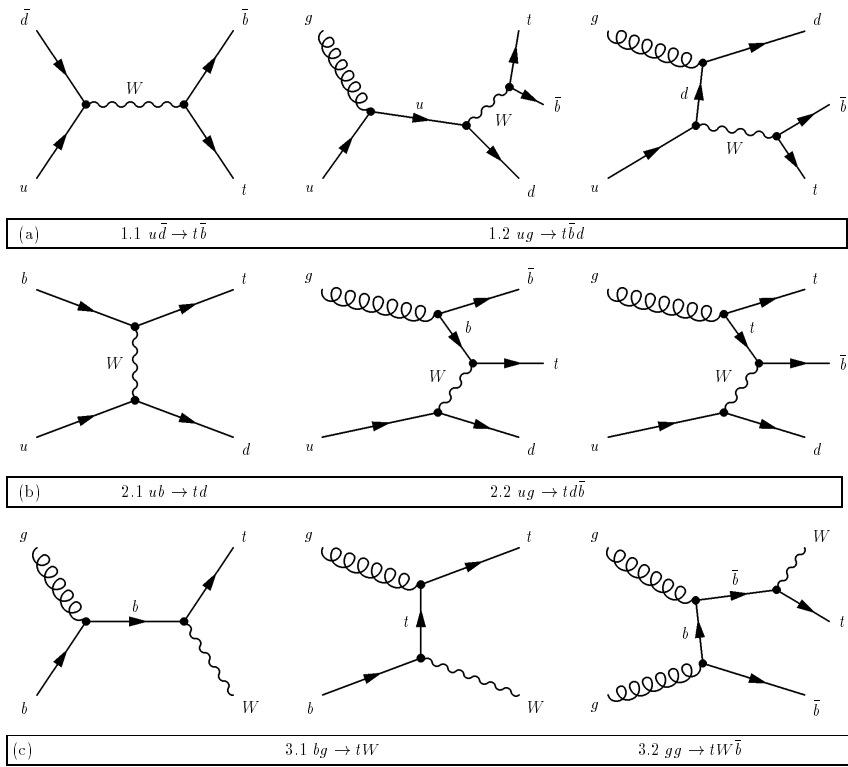


FIG. 1. Diagrams for single top production

It is necessary to stress that  $p\bar{p} \rightarrow tW + X$  process contributes only with 5% to the total cross section at the 2 TeV upgraded Tevatron. It could be easily omitted at Tevatron energies but should be taken into account for the LHC energies since as we shall demonstrate below its contribution at the LHC will be about 30% of the the total cross section of the single top quark production.

For events analysis we have rescaled the total cross sections of the single top production using the results of the NLO calculations from the papers [9] ( $m_t=175$  GeV):  
for  $\sqrt{s}=2$  TeV

$$\sigma(t\bar{b})=0.88 \pm 0.05 \text{ pb}, \sigma(Wg = tq\bar{b} + tq) = 2.43 \pm 0.4 \text{ pb};$$

and for  $\sqrt{s}=14 \text{ TeV}$

$$\sigma(t\bar{b})=10.2 \pm 0.6 \text{ pb}, \sigma(Wg = tq\bar{b} + tq) = 245 \pm 9 \text{ pb}.$$

We found LO cross section of  $p\bar{p} \rightarrow tW + X$  equal to 98 pb at the LHC with about 8% uncertainty due to a choice of different structure functions. The cross section for  $p\bar{p} \rightarrow tW^- + X$  was calculated using the following way. The process  $gg \rightarrow tW\bar{b}$  has been combined (diagram 3.2 in Fig. 1c shows the only one among 8 different topologies contributed to this subprocesses) with  $bg \rightarrow tW$  (diagram 3.1 in Fig. 1c). Similar to the  $W$ -gluon fusion process the subtraction of gluon splitting term has been made in order to avoid a double counting:

$$\sigma(gb + gg \rightarrow tW + X)_{real} = \sigma(gb \rightarrow tW) + \sigma(gg \rightarrow tW\bar{b}) - \sigma(g \rightarrow b\bar{b} \otimes gb \rightarrow tW) \quad (1)$$

In the previous studies the two above subprocess  $gg \rightarrow tW\bar{b}$  [10] and  $gb \rightarrow tW$  [11] have been considered separately which being simply added leads to an overestimation and stronger scale dependence of the cross section. In addition we calculated the complete set of Feynman diagrams for  $u\bar{u} + dd \rightarrow tW\bar{b}$  subprocesses.

However one should also take into account that the complete set of Feynman diagrams for  $Wtb$  processes includes  $t\bar{t}$  pair production subprocess. The  $t\bar{t}$  pair production is one the background processes included separately into analysis. Therefore its contribution has been removed from the  $tW + X$  rate. It can be done in a gauge invariant way by excluding the kinematical region of  $Wb$  invariant mass around top quark mass within 3 top decay widths as it was used in case of the  $e^+e^-$  collisions [12]:

$$M_t + 3\Gamma_{top} > M_{Wb} > M_t + 3\Gamma_{top}$$

. For our calculations we used:  $M_t = 175 \text{ GeV}$ ,  $\Gamma_{top} = 1.59 \text{ GeV}$ .

As a result, we have 91 pb for  $\sigma(gb + gg \rightarrow tW + X)_{real}$  process, while  $\sigma(u\bar{u} + dd \rightarrow tW\bar{b} + X)$  process gives additional 7 pb to the total  $p\bar{p} \rightarrow tW^- + X$  cross section which is therefore expected to be about 98 pb at LHC.

Thus the total single top rate is expected to be about 3.5 pb at the upgraded Tevatron and 350 pb at the LHC to be compared to the  $t\bar{t}$  production rate [13] 7.6 pb and 760 pb respectively. Relative contributions of different subprocesses to the total single top quark production cross section at Tevatron are the following :

$$p\bar{p} \rightarrow tqbb(39\%),$$

$$p\bar{p} \rightarrow tb(30\%),$$

$$p\bar{p} \rightarrow tq(26\%),$$

$$p\bar{p} \rightarrow tW + X (5\%).$$

Relative contribution of  $p\bar{p} \rightarrow tb$  and  $p\bar{p} \rightarrow tW + X$  turn over at LHC:

$$p\bar{p} \rightarrow tq\bar{b}(44.2\%),$$

$$p\bar{p} \rightarrow tb(2.8\%),$$

$$p\bar{p} \rightarrow tq(25\%),$$

$$p\bar{p} \rightarrow tW + X (28\%).$$

As it was mentioned we consider here the leptonic decay modes of  $W$ -boson from the top quark and therefore the final state signature to search for the signal will be:

$$e^\pm(\mu^\pm) + \cancel{E}_T + 2(3)jets$$

where one of the jets is the  $b$ -quark jet from the top-quark decay.

## B. Main backgrounds

The main backgrounds leading to the same  $e^\pm(\mu^\pm) + \cancel{E}_T + 2(3)jets$  final state signature as the single top signal are the following:  $p\bar{p} \rightarrow W + 2(3)jets$  (gluonic,  $\alpha\alpha_s$  order and electroweak  $\alpha^2$  order)),  $p\bar{p} \rightarrow t\bar{t}$  pair top quark production and  $j(j)b\bar{b}$  QCD fake background when one jet imitates the electron.

All numbers for  $Wjj(Wb\bar{b})$  and  $j(j)b\bar{b}$  backgrounds are presented below for the initial general cuts on jets:

$$\Delta R_{jj(ej)} > 0.5, p_{tjet} > 10 \text{ GeV} \text{ for Tevatron};$$

$$\Delta R_{jj(ej)} > 0.5, p_{tjet} > 20 \text{ GeV} \text{ for LHC}.$$

Total cross section of  $W+2jets$  'gluonic' background is more than 2 orders of magnitude higher than the signal one. This process includes 32 subprocesses for  $u, d$ -quarks and gluons in the initial state [14], and the total cross section equals to 1240 pb for Tevatron and 7500 pb for LHC ( $s$ - and  $c$ - sea quarks give additional 3% contribution to the total cross section).

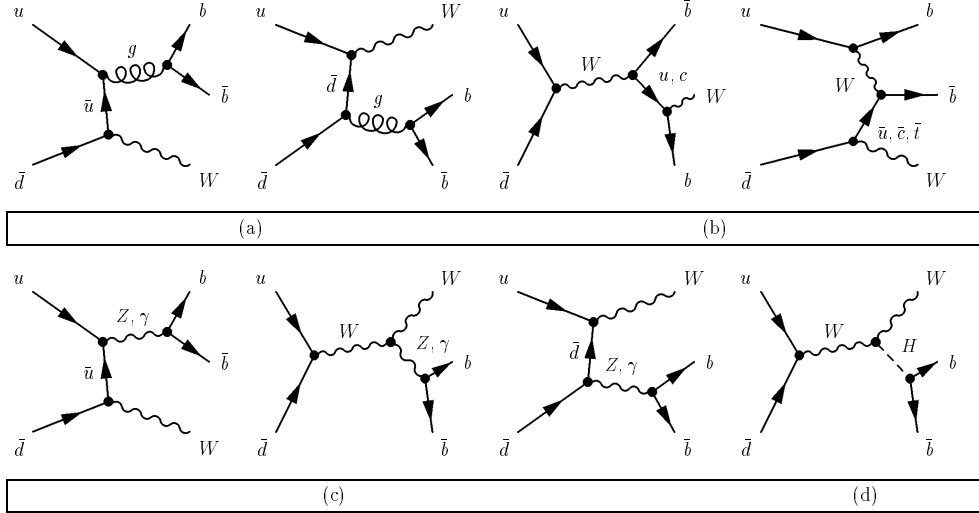


FIG. 2. Diagrams for  $Wb\bar{b}$  background

The specific feature of the single top production is the high energetic  $b$ -jet in final state and one additional  $b$ -jet for  $W$ -gluon and  $W^*$  processes. It is clear that the only chance to extract the signal from such an overwhelming background is the efficient  $b$ -quark identification. We assume 50% of a double  $b$ -tagging efficiency hereafter.

However the cross section of the  $W + 2jet$  process is so large that even with the requirement of a double  $b$ -tagging but due to a  $b$ -quark jet misidentification it represents an important part of the total background. In our study we chose 0.5% misidentification probability which based on the previous MC analysis [15].

The  $b$ -quark content of the  $W + 2jet$  processes is fairly small – less then 1%. For the cuts mentioned above the total cross section for  $W^\pm b\bar{b}$  process(gluon splitting) is 8.7 pb for Tevatron and 30 pb for LHC. However, the  $W + 2b - jet$  process is the irreducible part of the total background which has different kinematical properties from the main QCD  $W + 2jet$  part, and as will be shown below it depends differently on the cuts.

Therefore the  $W^\pm b\bar{b}$  background has been considered separately and we have calculated it completely.

Complete set of Feynman background diagrams for  $Wb\bar{b}$  final state is shown in Fig. 2 for  $u-$  and  $\bar{d}$ -quarks in the initial state. The main contribution comes from subprocess (a) with the gluon splitting into the  $b\bar{b}$  quark pair. Diagrams with virtual photon (c) contribute only 1% to the total cross section. Contribution from  $WZ$  process (c) can be suppressed by applying cut on the invariant  $b\bar{b}$ -mass. LO cross section for  $WZ$  is 2.5 pb at Tevatron and about 30 pb at LHC. For our analysis we apply K-factor=1.33 (1.55) for Tevatron(LHC) to rescale this number for the NLO total cross section [16]. Cross section of the process (d) of Higgs production (we take as an example  $m_H = 110$  GeV) is even smaller: 0.16 (1.8) pb (LO) at Tevatron (LHC), and it means the Higgs is really not an important background for the single top. We apply K-factor=1.25 (1.1) for Tevatron(LHC) to rescale the results for NLO one [17]. Diagrams (b) give very small contribution due to small value of CKM elements.

process	Tevatron (pb)	LHC (pb)
$gg \rightarrow gbb$	$1.64 \cdot 10^3$	$3.91 \cdot 10^3$
$g\bar{u}(\bar{u}g) \rightarrow \bar{u}b\bar{b}$	$1.80 \cdot 10^4 (2.50 \cdot 10^3)$	$5.61 \cdot 10^3 (5.61 \cdot 10^3)$
$gu(ug) \rightarrow ub\bar{b}$	$2.50 \cdot 10^4 (1.80 \cdot 10^4)$	$2.41 \cdot 10^4 (2.41 \cdot 10^4)$
$g\bar{d}(\bar{d}g) \rightarrow db\bar{b}$	$9.00 \cdot 10^3 (3.21 \cdot 10^3)$	$6.61 \cdot 10^3 (6.61 \cdot 10^3)$
$g\bar{s}(\bar{s}g) \rightarrow sb\bar{b}$	$1.97 \cdot 10^3 (1.97 \cdot 10^3)$	$4.49 \cdot 10^3 (4.49 \cdot 10^3)$
$gd(dg) \rightarrow db\bar{b}$	$3.21 \cdot 10^3 (9.00 \cdot 10^3)$	$1.38 \cdot 10^4 (1.38 \cdot 10^4)$
$gs(sg) \rightarrow sb\bar{b}$	$1.97 \cdot 10^3 (1.97 \cdot 10^3)$	$4.49 \cdot 10^3 (4.49 \cdot 10^3)$
$d\bar{d}(\bar{d}d) \rightarrow gb\bar{b}$	$5.67 \cdot 10^2 (1.25 \cdot 10^2)$	$2.82 \cdot 10^2 (2.82 \cdot 10^2)$
$u\bar{u}(\bar{u}u) \rightarrow gb\bar{b}$	$1.31 \cdot 10^3 (8.61 \cdot 10^1)$	$4.16 \cdot 10^2 (4.16 \cdot 10^2)$
Total	$2.40 \cdot 10^5$ pb	$5.11 \cdot 10^5$ pb

TABLE I. Total cross section for  $jj\bar{b}\bar{b}$  process for Tevatron and LHC. The following cuts have been applied at the parton level calculations:  $\Delta R_{jj} > 0.5$ ,  $p_{t,jet} > 10$  GeV for Tevatron and  $\Delta R_{jj(ej)} > 0.5$ ,  $p_{t,jet} > 20$  GeV for LHC

An important background is top-quark pair production: when one of the top decays hadronically and another one – leptonically. One of the cut which helps to reduce the background is the cut on the number of jets which was required to be less than four. At the parton level this cut reduces the top pair rate very strongly. However at the simulation level with a hadronization and jet reconstruction being taken into account the reduction of this background is not so strong anymore. And as a result the top-quark pair represents an important part of the background. This fact will be shown below. NLO total cross section for tt-pair production was taken [13] at Tevatron to be equal to 7.56 pb and 760 pb at LHC.

process	Tevatron (pb)	LHC (pb)
$uu \rightarrow uubb$	$1.23 \cdot 10^2$	$1.17 \cdot 10^3$
$u\bar{u}(u\bar{u}) \rightarrow b\bar{b}b\bar{b}$	$2.55 \cdot 10^0$	$1.06 \cdot 10^0 (1.06 \cdot 10^0)$
$u\bar{u}(u\bar{u}) \rightarrow s\bar{s}b\bar{b}$	$6.61 \cdot 10^0$	$2.53 \cdot 10^0 (2.53 \cdot 10^0)$
$u\bar{u}(u\bar{u}) \rightarrow c\bar{c}b\bar{b}$	$6.52 \cdot 10^0$	$2.53 \cdot 10^0 (2.53 \cdot 10^0)$
$u\bar{u}(u\bar{u}) \rightarrow d\bar{d}b\bar{b}$	$6.66 \cdot 10^0$	$2.52 \cdot 10^0 (2.53 \cdot 10^0)$
$u\bar{u}(u\bar{u}) \rightarrow u\bar{u}b\bar{b}$	$8.70 \cdot 10^2$	$3.38 \cdot 10^2 (3.38 \cdot 10^2)$
$u\bar{u}(u\bar{u}) \rightarrow gg\bar{b}\bar{b}$	$2.15 \cdot 10^2$	$8.92 \cdot 10^1 (8.92 \cdot 10^1)$
$ud(du) \rightarrow u\bar{d}b\bar{b}$	$1.44 \cdot 10^2 (4.20 \cdot 10^1)$	$7.40 \cdot 10^2 (7.40 \cdot 10^2)$
$us(su) \rightarrow u\bar{s}b\bar{b}$	$9.63 \cdot 10^1$	$1.71 \cdot 10^2 (1.71 \cdot 10^2)$
$u\bar{d}(d\bar{u}) \rightarrow u\bar{d}b\bar{b}$	$3.73 \cdot 10^2 (1.20 \cdot 10^2)$	$3.74 \cdot 10^2 (3.74 \cdot 10^2)$
$u\bar{s}(\bar{s}u) \rightarrow u\bar{s}b\bar{b}$	$9.63 \cdot 10^1$	$1.71 \cdot 10^2 (1.71 \cdot 10^2)$
$d\bar{u}(\bar{u}d) \rightarrow d\bar{u}b\bar{b}$	$3.73 \cdot 10^2 (1.20 \cdot 10^2)$	$1.78 \cdot 10^2 (1.78 \cdot 10^2)$
$s\bar{u}(\bar{u}s) \rightarrow \bar{u}s\bar{b}\bar{b}$	$9.63 \cdot 10^1$	_____
$\bar{u}\bar{u} \rightarrow \bar{u}\bar{u}b\bar{b}$	$9.10 \cdot 10^1$	_____
$\bar{u}\bar{d}(\bar{d}\bar{u}) \rightarrow \bar{u}\bar{d}b\bar{b}$	$4.20 \cdot 10^1 (1.44 \cdot 10^2)$	_____
$\bar{u}\bar{s}(\bar{s}\bar{u}) \rightarrow \bar{u}\bar{s}b\bar{b}$	_____ $(9.63 \cdot 10^1)$	_____
$dd \rightarrow d\bar{d}b\bar{b}$	$6.40 \cdot 10^1$	$1.17 \cdot 10^3$
$d\bar{d}(d\bar{d}) \rightarrow b\bar{b}b\bar{b}$	$9.38 \cdot 10^{-1} (9.38 \cdot 10^{-1})$	$7.00 \cdot 10^{-1} (7.00 \cdot 10^{-1})$
$d\bar{d}(d\bar{d}) \rightarrow s\bar{s}b\bar{b}$	$2.40 \cdot 10^0 (2.40 \cdot 10^0)$	$1.70 \cdot 10^0 (1.70 \cdot 10^0)$
$d\bar{d}(d\bar{d}) \rightarrow c\bar{c}b\bar{b}$	$2.35 \cdot 10^0 (2.35 \cdot 10^0)$	$1.70 \cdot 10^0 (1.70 \cdot 10^0)$
$d\bar{d}(d\bar{d}) \rightarrow d\bar{d}b\bar{b}$	$2.24 \cdot 10^2 (2.24 \cdot 10^2)$	$2.05 \cdot 10^2 (2.05 \cdot 10^2)$
$d\bar{d}(d\bar{d}) \rightarrow u\bar{u}b\bar{b}$	$2.40 \cdot 10^0 (2.40 \cdot 10^0)$	$1.70 \cdot 10^0 (1.70 \cdot 10^0)$
$d\bar{d}(\bar{d}d) \rightarrow gg\bar{b}\bar{b}$	$7.30 \cdot 10^1 (7.30 \cdot 10^1)$	$5.86 \cdot 10^1 (5.86 \cdot 10^1)$
$\bar{d}\bar{d} \rightarrow \bar{d}\bar{d}b\bar{b}$	$5.10 \cdot 10^1$	_____
$d\bar{s}(\bar{s}d) \rightarrow d\bar{s}b\bar{b}$	$4.23 \cdot 10^1$	$9.16 \cdot 10^1 (9.16 \cdot 10^1)$
$ds(s\bar{d}) \rightarrow ds\bar{b}\bar{b}$	$4.23 \cdot 10^1$	$9.16 \cdot 10^1 (9.16 \cdot 10^1)$
$\bar{d}\bar{s}(\bar{s}\bar{d}) \rightarrow \bar{d}\bar{s}b\bar{b}$	_____ $4.23 \cdot 10^1$	$9.16 \cdot 10^1 (9.16 \cdot 10^1)$
$\bar{d}\bar{s}(\bar{s}\bar{d}) \rightarrow \bar{d}\bar{s}b\bar{b}$	_____ $4.23 \cdot 10^1$	$9.16 \cdot 10^1 (9.16 \cdot 10^1)$
$gu(ug) \rightarrow gub\bar{b}$	$7.28 \cdot 10^2 (7.82 \cdot 10^3)$	$2.37 \cdot 10^4 (2.37 \cdot 10^4)$
$g\bar{u}(\bar{u}g) \rightarrow g\bar{u}b\bar{b}$	$7.82 \cdot 10^3 (7.28 \cdot 10^2)$	$4.53 \cdot 10^3 (4.53 \cdot 10^3)$
$gd(dg) \rightarrow g\bar{d}b\bar{b}$	$1.01 \cdot 10^3 (3.52 \cdot 10^3)$	$1.29 \cdot 10^4 (1.29 \cdot 10^4)$
$gs(sg) \rightarrow g\bar{s}b\bar{b}$	$7.61 \cdot 10^2 (7.61 \cdot 10^2)$	$2.43 \cdot 10^3 (2.43 \cdot 10^3)$
$g\bar{d}(\bar{d}g) \rightarrow g\bar{d}b\bar{b}$	$3.52 \cdot 10^3 (1.01 \cdot 10^3)$	$5.47 \cdot 10^3 (5.47 \cdot 10^3)$
$g\bar{s}(\bar{s}g) \rightarrow g\bar{s}b\bar{b}$	$7.61 \cdot 10^2 (7.61 \cdot 10^2)$	$2.43 \cdot 10^3 (2.43 \cdot 10^3)$
$gg \rightarrow b\bar{b}b\bar{b}$	$9.90 \cdot 10^1$	$6.58 \cdot 10^2$
$gg \rightarrow s\bar{s}b\bar{b}$	$4.80 \cdot 10^2$	$2.21 \cdot 10^3$
$gg \rightarrow c\bar{c}b\bar{b}$	$4.60 \cdot 10^2$	$2.24 \cdot 10^3$
$gg \rightarrow d\bar{d}b\bar{b}$	$3.85 \cdot 10^2$	$2.11 \cdot 10^3$
$gg \rightarrow u\bar{u}b\bar{b}$	$3.85 \cdot 10^2$	$2.11 \cdot 10^3$
$gg \rightarrow g\bar{g}b\bar{b}$	$3.62 \cdot 10^4$	$2.43 \cdot 10^5$
Total	$7.01 \cdot 10^4$ pb	$3.62 \cdot 10^5$ pb

TABLE II. Total cross section for  $jjb\bar{b}$  process for Tevatron and LHC. The following cuts have been applied at the parton level calculations:  $\Delta R_{jj} > 0.5$ ,  $p_{t,jet} > 10$  GeV for Tevatron and  $\Delta R_{jj(ej)} > 0.5$ ,  $p_{t,jet} > 20$  GeV for LHC

Another kind of the important reducible background comes from the multijet QCD processes. This happens due to a possible misidentification of jet as an electron in the detector. Though the probability of that is very small (of order of 0.01-0.03%) [18], the cross section for such processes is huge and give a significant contribution to the background for single top production. For the analysis we took  $\epsilon_{fake}=0.02\%$ .

We have calculated the total cross section and made MC simulation for  $jjb$  and  $jjbb$  processes which are relevant for our signature if one the light jet imitates electron. In such a way we could simulate the basic distributions of the expected fake background and understand how strong it could be suppressed by kinematical cuts. The MC simulation of the fake background for the single top study is presented for a first time.

The background from the light jets is appeared to be less important despite on the fact the light jet cross sections even with cuts are very large. The light jet background is suppressed by three small factors, by double mistag probability to identify light jet as a b-jet and by the small fake probability to identify light jet as an electron. For instance the  $gg \rightarrow ggg$  subprocess could contribute to the background when two gluon jets fake b-quark jets and a third gluon jet fakes the lepton. The cross section of  $gg \rightarrow ggg$  itself is huge but as was mentioned it's contribution to the single top background is suppressed by fake probability of gluon multiplied by double mistag probability of two gluons. For example, the cross section of triple gluon production Tevatron is  $2.7 \cdot 10^7$  pb, double mistag gluon probability is equal to  $10^{-6}$ , fake probability of gluon is of order  $10^{-4}$ . Therefore the contribution from  $gg \rightarrow ggg$  process is estimated to be equal to  $\simeq 10^{-2}$  pb (we use combinatoric factor 3 here) and one can neglect it.

In the Table I and Table II all subprocesses giving  $jjb$  and  $jjbb$  final state signature are shown respectively with the corresponding cross sections for the Tevatron and LHC. In our calculations we neglected the double sea quark and  $c$ -sea quark small contributions. Total cross section for  $jjb$  at the Tevatron (LHC) is 240 and 70 (511 and 362) nb for  $jjb$  and  $jjbb$ .

The cross section of the  $jjb$  process in the Table I is only about 2 times higher at LHC than at Tevatron because higher jet  $p_T$  cuts for LHC have been used (20 GeV at LHC and 10 GeV at Tevatron). If the equal jet  $p_T$  cuts are used the cross section at LHC is about 50 times higher than that at Tevatron.

We performed two ways of calculation of the  $jjb\bar{b}$  process, the complete tree level calculation and the splitting approximation when one uses the complete result from  $jjb\bar{b}$  with an additional jet radiation from the initial and final states. In such a way we have checked the validity of splitting approximation.

As it was expected the splitting approximation works reasonably well for the total rate if rather soft cuts on the additional jet are used and the difference increases if the more strong cuts are applied. The Table III illustrates such a difference in results for the approximation and exact calculations for various cuts on the  $p_T$  of the second jet (that is the light jet with the smallest  $p_T$  which is more likely an additional radiated light jet).

$p_{j2T} [GeV]$	10	15	20	40
$\sigma_{jjbb}^{exact} [pb]$	70	32	14	1.2
$\sigma_{jjbb}^{split} [pb]$	64	22	8	0.25

TABLE III. Comparison the cross sections for  $jjb\bar{b}$  process for exact calculations and the splitting approximation for various  $p_{j2T}$  cuts at Tevatron. The following cuts have been applied at the MC level:  $\Delta R_{jj} > 0.5$ ,  $p_t$  of the first jet  $> 10$  GeV

Indeed one can see that for  $p_{j2T} > 10$  GeV cut the difference between exact calculation and the splitting approximation is only about 10 %: 70 nb and 64 nb respectively. But after  $p_{j2T} > 40$  GeV cut those results differ almost by factor 5: one has 1.2 and 0.25 nb for exact calculation of  $jjb\bar{b}$  and splitting approximation respectively.

The expected difference in the distribution on the momenta transverse of the second jet is illustrated in Figure 3. The distribution in case of the splitting approximation is significantly softer.

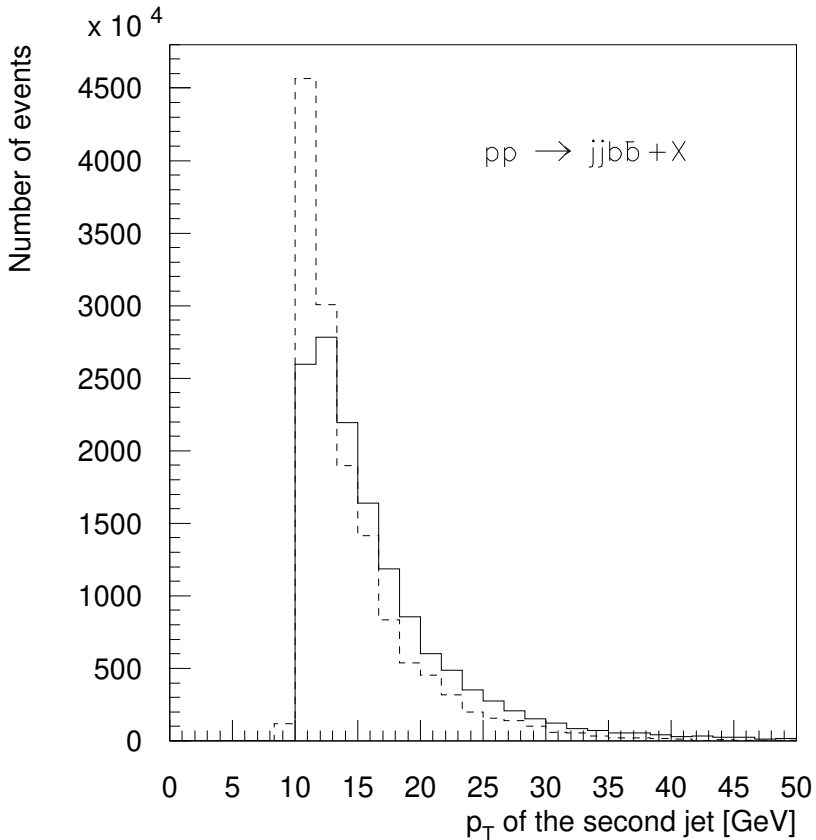


FIG. 3. Distribution for  $p_T$  of the second jet for  $jjb\bar{b}$  process for exact calculation (solid line) and for splitting from  $jb\bar{b}$  process (dashed line) at Tevatron.

Since we do not apply high  $p_T$  cut on jet (one of them fakes electron, for which we apply 15 GeV  $p_T$  cut) the difference between exact calculation and the approximation is of order of 25% for the fake background simulation.

### C. Signal and background kinematical properties

The rate of the signal and backgrounds presented above clearly shows that even after  $b$ -tagging the signal is still more than one order less than the background. This fact requires a special kinematical analysis in order to find out a strategy how to suppress the background and extract the signal in an optimal way.

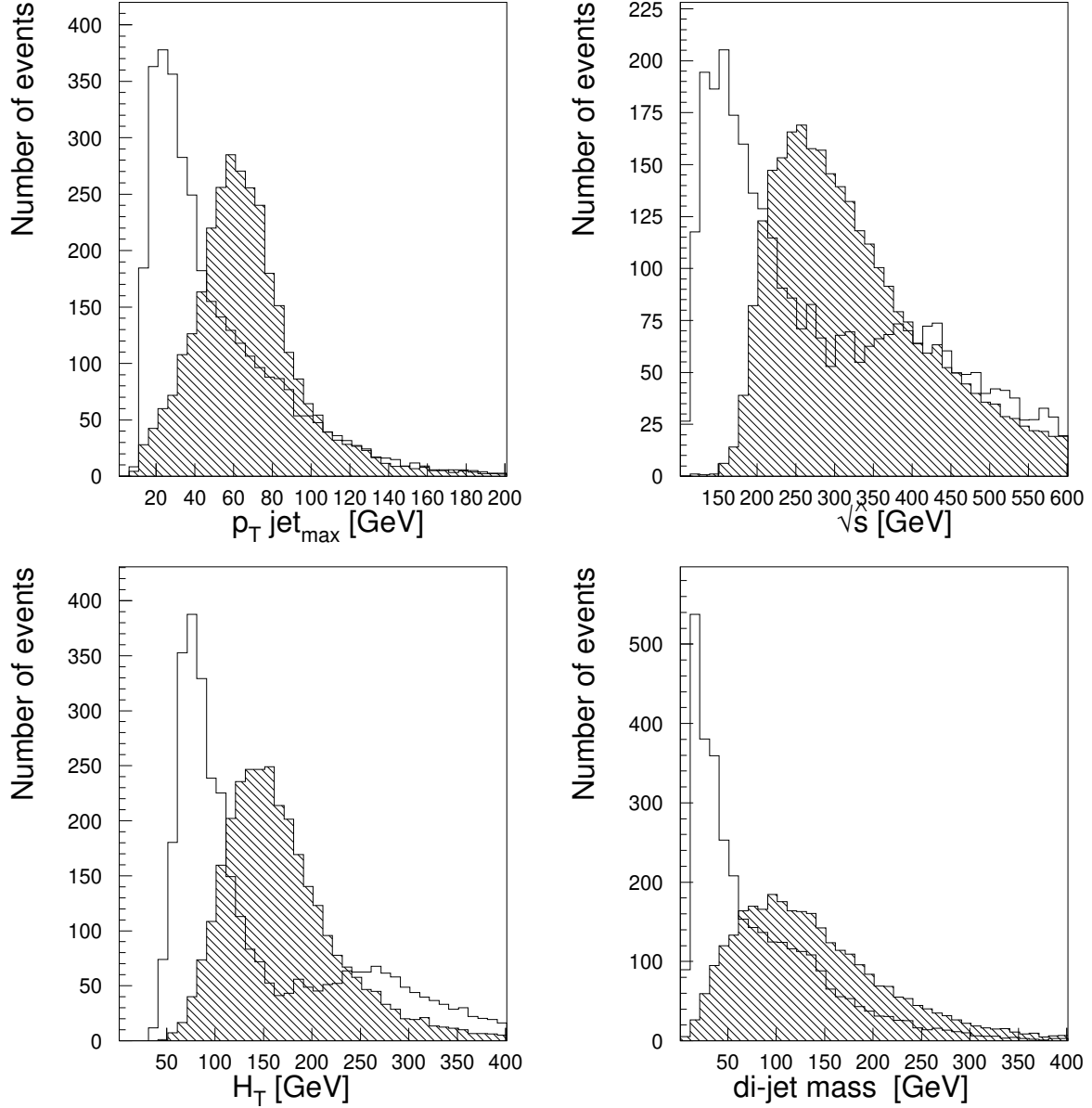


FIG. 4. Distributions for signal and background for the some most spectacular variables at Tevatron. Sketched histogram stands for signal.

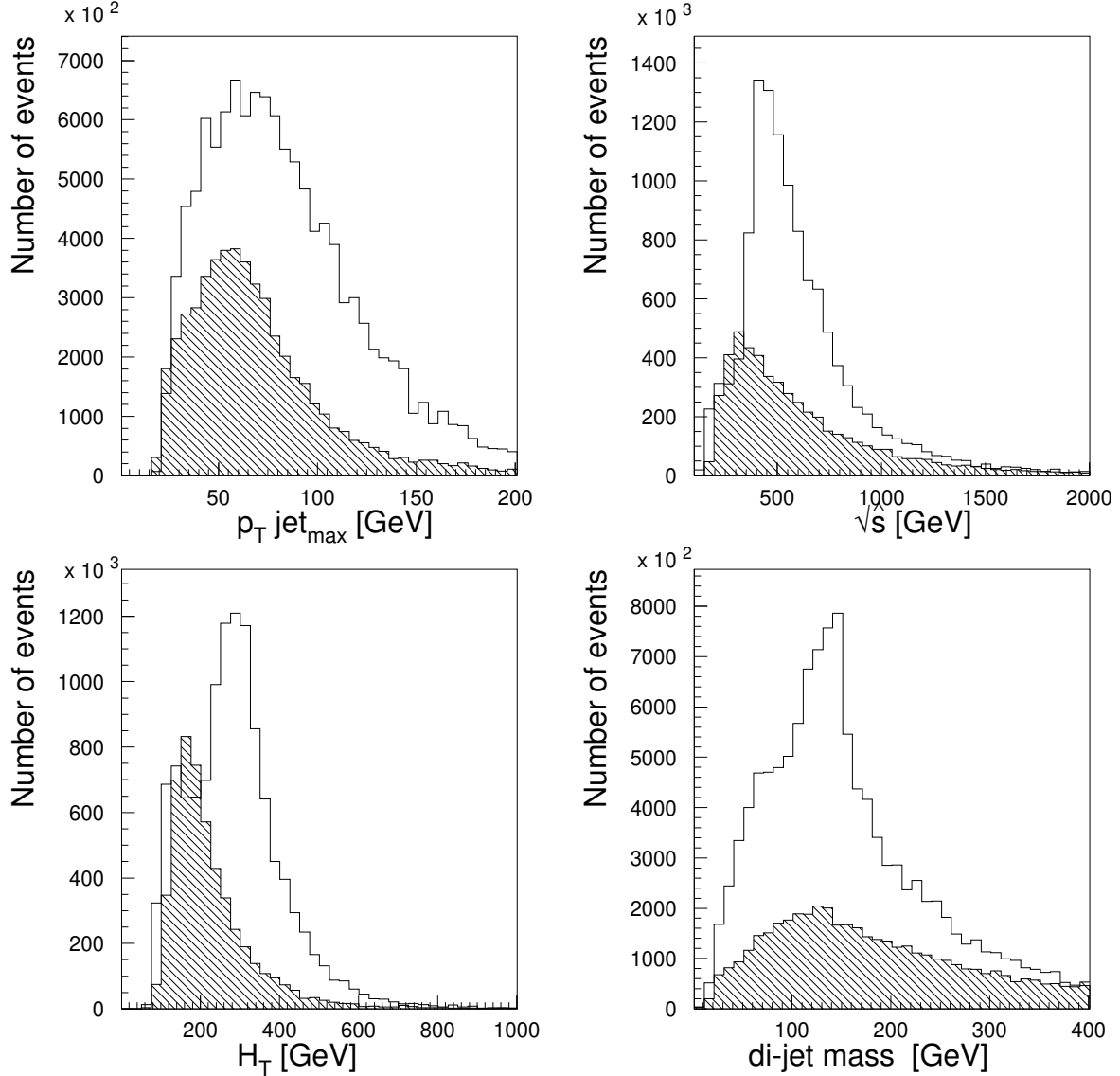


FIG. 5. Distributions for signal and background for the some most spectacular variables at LHC. Sketched histogram stands for signal.

The distributions for several sensitive kinematical variables for a separation of the signal and the background are shown in Fig. 4 for the Tevatron and in Fig. 5 for the LHC. The mentioned above effects of the jet fragmentation, detector resolution and energy smearing are included in the figures. Among the kinematical variables for separation of the signal and background the most attractive were found to be:

- $p_T$  of leading jet:  
 $p_T$  of leading jet distribution for the signal has a peak around  $m_{top}/3$ , while it is much softer for QCD background at Tevatron (Fig. 4). The main difference between kinematical distributions for signal and background at Tevatron is that jets from  $W + jj$  and  $j(j)bb$  processes are softer and less central than those for signal with one very hard jet coming from top and another softer jet, accompanying top quark. For LHC there is no such striking difference in  $p_T$  of leading jet distribution between signal and background. It happens because of higher CM energy and dominating contribution to the background from  $t\bar{t}$  production (Fig. 5)
- $\sqrt{s}$  - invariant mass of the system (Fig. 4,5):  
it is always bigger for signal than those for  $Wjj$  and  $j(j)bb$  backgrounds. It is important to notice that  $t\bar{t}$  background peaks at higher values of invariant mass of the system which is clearly seen in the case of LHC, where this background dominates.

- $p_T W$ :  $W$  boson tends to be harder from top-quark decay than from QCD processes.
- scalar transverse energy  $H_T$  (Fig. 4c,5c),  $H_T = |E_T(\text{jet1})| + |E_T(\text{jet2})| + |E_T(\text{lepton})|$  : this kinematical variable has peak around 150 GeV for signal, around 300 GeV for  $t\bar{t}$  background and peaks at the small values for QCD background.
- di-jet mass (Fig. 4,5):  
It is harder for signal than for QCD background, for which  $b\bar{b}$ -pair coming mainly from gluon splitting, in the same time di-jet mass distribution of  $t\bar{t}$  background has similar shape with the signal. Di-jet mass cut is also used for a reduction of  $WZ$  background.

In our analysis we used "effective" invariant top quark mass variable which is constructed using the following algorithm. It is clear that mass of the top quark decaying to lepton, neutrino and b-quark can not be unambiguously reconstructed since z-component of neutrino can not be measured. One can construct top quark mass

$$m_t^2 = (P_e + P_\nu + P_b)^2 \quad (2)$$

using, one of two solutions for  $p_{z\nu}$  of simple quadratic equation <sup>1</sup>

$$m_W^2 = (P_e + P_\nu)^2 = 80.12^2 \quad (3)$$

Our Monte Carlo analysis shows that if one chooses  $p_{z\nu}$  to be the  $|p_{z\nu}|_{\min}$  from two solutions than it will be in about 70% true  $p_{z\nu}$ . In fact the reason for that is obvious and related to the fact that smaller values of  $p_{z\nu}$  correspond in most cases to smaller values of the total invariant mass  $\sqrt{s}$ . And for the smaller values of  $\sqrt{s}$  the effective parton-parton luminosity is larger and therefore the cross section is higher. However anyway if the one solution for  $p_{z\nu}$  is used the invariant "effective" mass distribution is broader than real invariant top quark mass and one should apply rather wide window for this kinematical variable in order not to lose too much signal events. We chose  $\pm 50$  GeV window in our analysis.

Based on such different behaviors of the signal and background kinematical distributions the following set of cuts for the background suppression has been worked out:

Cut 1:  $\Delta R_{jj(ej)} > 0.5$ ,  $p_{T\text{jet}} > 10$  GeV,  $\not{E}_T > 15$  GeV,  $p_{te} > 15$  GeV for Tevatron and  $\Delta R_{jj(ej)} > 0.5$ ,  $p_{T\text{jet}} > 20$  GeV,  $\not{E}_T > 20$  GeV,  $p_{te} > 20$  GeV for LHC which are "initial" cuts for jet separation and  $W$ -boson identification

Cut 2:  $p_{T\text{jet, max}} > 45$  GeV

Cut 3:  $\sqrt{s} > 180$  GeV

Cut 4:  $p_T W > 30$  GeV

Cut 5: di-jet mass  $> 25$  GeV

Cut 6:  $H_T > 100$  GeV for Tevatron and  $260 > H_T > 100$  GeV for LHC

Cut 7:  $3 \geq n\text{-jet} \geq 2$

Cut 8: di-jet mass  $\geq 40$  GeV

The effect of the consequent application of this set of cuts is presented in Table IV,V. We should stress that "effective" mass window cut  $\pm 50$  GeV was an initial cut and has been applied along with all others cuts shown in the table.

Number of events presented in the tables as well as in the Figs. 4,5 corresponds to the total integrated luminosity  $2 \text{ fb}^{-1}$  ( $100 \text{ fb}^{-1}$ ) <sup>2</sup> for Tevatron (LHC) under the mentioned above assumptions of double  $b$ -tagging efficiency 50% and  $b$ -quark mistagging probability 0.5%.

cuts	signal	$Wbb$	$Wjj$	$WZ$	$j(j)bb$	$t\bar{t}$	$WH$
Cut 1	$1.986 \cdot 10^2$	$3.680 \cdot 10^2$	$2.644 \cdot 10^2$	$2.059 \cdot 10^1$	$6.292 \cdot 10^2$	$5.849 \cdot 10^2$	$8.428 \cdot 10^0$
Cut 2	$1.514 \cdot 10^2$	$1.711 \cdot 10^2$	$1.034 \cdot 10^2$	$1.136 \cdot 10^1$	$1.114 \cdot 10^2$	$4.898 \cdot 10^2$	$6.491 \cdot 10^0$
Cut 3	$1.493 \cdot 10^2$	$1.453 \cdot 10^2$	$9.211 \cdot 10^1$	$1.053 \cdot 10^1$	$1.030 \cdot 10^2$	$4.898 \cdot 10^2$	$6.278 \cdot 10^0$

<sup>1</sup>Such a method of the single top quark mass reconstruction is known and has been used in the past (see, C.-P. Yuan, Phys. Rev. D **41**, 42 (1990))

<sup>2</sup>The numbers for the LHC could be easily rescaled to the  $30 \text{ fb}^{-1}$  of the low luminosity LHC operation.

Cut 4	$1.295 \cdot 10^2$	$1.173 \cdot 10^2$	$7.687 \cdot 10^1$	$8.564 \cdot 10^0$	$8.910 \cdot 10^1$	$4.191 \cdot 10^2$	$5.145 \cdot 10^0$
Cut 5	$1.286 \cdot 10^2$	$1.107 \cdot 10^2$	$7.488 \cdot 10^1$	$8.515 \cdot 10^0$	$8.353 \cdot 10^1$	$4.186 \cdot 10^2$	$5.124 \cdot 10^0$
Cut 6	$1.249 \cdot 10^2$	$1.038 \cdot 10^2$	$6.649 \cdot 10^1$	$8.087 \cdot 10^0$	$6.961 \cdot 10^1$	$4.185 \cdot 10^2$	$5.013 \cdot 10^0$
Cut 7	$1.247 \cdot 10^2$	$1.031 \cdot 10^2$	$6.649 \cdot 10^1$	$7.419 \cdot 10^0$	$4.455 \cdot 10^1$	$1.055 \cdot 10^2$	$4.562 \cdot 10^0$
Cut 8	$1.216 \cdot 10^2$	$8.867 \cdot 10^1$	$6.141 \cdot 10^1$	$7.266 \cdot 10^0$	$3.619 \cdot 10^1$	$1.039 \cdot 10^2$	$4.490 \cdot 10^0$
Signal: 122, Background: 297; S/B $\simeq 0.41$							

TABLE IV. Number of events for single top signal and background at Tevatron. Cuts numbering correspond to (4) set of cuts with their consequent application. Window  $\pm 50$  GeV around 175 GeV bin was imposed for reconstructed "effective" top mass.

cuts	signal	$Wbb$	$Wjj$	$WZ$	$j(j)bb$	$t\bar{t}$	$WH$
Cut 1	$1.212 \cdot 10^6$	$8.236 \cdot 10^4$	$1.724 \cdot 10^5$	$1.912 \cdot 10^4$	$1.155 \cdot 10^6$	$4.449 \cdot 10^6$	$6.124 \cdot 10^3$
Cut 2	$8.792 \cdot 10^5$	$5.143 \cdot 10^4$	$1.058 \cdot 10^5$	$1.177 \cdot 10^4$	$6.112 \cdot 10^5$	$3.762 \cdot 10^6$	$4.923 \cdot 10^3$
Cut 3	$8.764 \cdot 10^5$	$4.871 \cdot 10^4$	$1.015 \cdot 10^5$	$1.138 \cdot 10^4$	$6.053 \cdot 10^5$	$3.762 \cdot 10^6$	$4.854 \cdot 10^3$
Cut 4	$7.423 \cdot 10^5$	$3.826 \cdot 10^4$	$7.758 \cdot 10^4$	$9.048 \cdot 10^3$	$4.974 \cdot 10^5$	$3.262 \cdot 10^6$	$3.976 \cdot 10^3$
Cut 5	$7.401 \cdot 10^5$	$3.771 \cdot 10^4$	$7.735 \cdot 10^4$	$9.013 \cdot 10^3$	$4.957 \cdot 10^5$	$3.262 \cdot 10^6$	$3.972 \cdot 10^3$
Cut 6	$5.643 \cdot 10^5$	$3.649 \cdot 10^4$	$7.524 \cdot 10^4$	$7.545 \cdot 10^3$	$4.729 \cdot 10^5$	$6.214 \cdot 10^5$	$3.334 \cdot 10^3$
Cut 7	$5.370 \cdot 10^5$	$3.610 \cdot 10^4$	$7.408 \cdot 10^4$	$6.122 \cdot 10^3$	$2.411 \cdot 10^5$	$1.886 \cdot 10^5$	$2.740 \cdot 10^3$
Cut 8	$5.296 \cdot 10^5$	$3.177 \cdot 10^4$	$7.019 \cdot 10^4$	$6.030 \cdot 10^3$	$2.301 \cdot 10^5$	$1.886 \cdot 10^5$	$2.694 \cdot 10^3$
Signal: $5.3 \cdot 10^5$ , Background: $5.3 \cdot 10^5$ ; S/B = 1.0							

TABLE V. Number of events for single top signal and background at LHC. Cuts numbering correspond to (4) set of cuts with their consequent application. Window  $\pm 50$  GeV around 175 GeV bin was imposed for reconstructed "effective" top mass.

From the tables one can see that in fact two cuts, Cut 2 reducing the  $QCD + Wjj$  background and Cut 7 eliminating  $t\bar{t}$  background, play the leading role. In the same time all cuts are strongly correlated and one can effectively replace Cut 2 by Cut3+4 or more complicated combination with the same success.

The strong background reduction is clearly illustrated in Fig. 6a,b,7a,b for the invariant top mass distribution before (a) and after (b) application of kinematical cuts. After cuts applied the background became about 10 times smaller at the Tevatron and 18 times at the LHC while approximately 60% (40%) of signal survived at Tevatron (LHC). Signal/background ratio becomes equal approximately to 0.4 at Tevatron and 1 at LHC. Such a background suppression will allow to measure the signal cross section with the high accuracy.

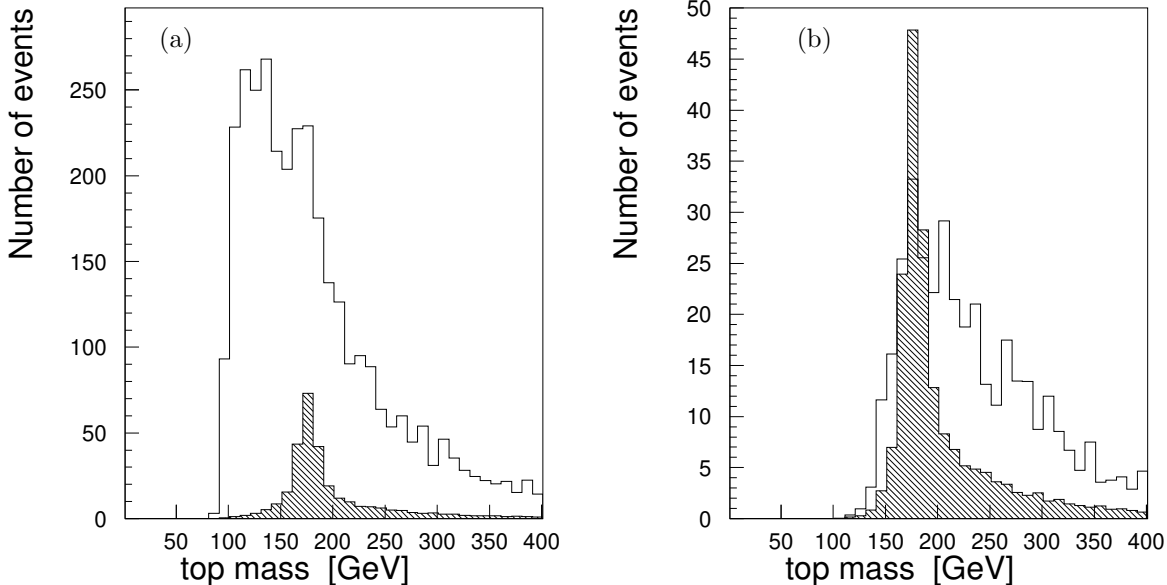


FIG. 6. Distributions for invariant top mass before (a) and after (b) cut application at Tevatron. Sketched histogram stands for signal.

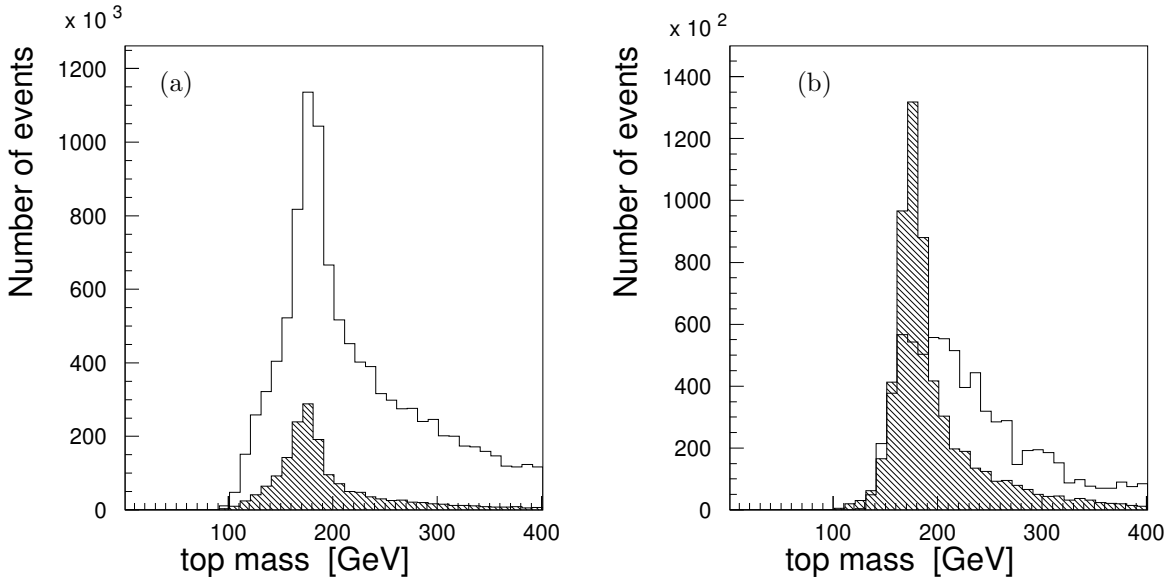


FIG. 7. Distributions for invariant top mass before (a) and after (b) cut application at LHC. Sketched histogram stands for signal.

The cross section for single top quarks includes the  $Wtb$  coupling directly, in contrast to  $t\bar{t}$  pair production. Therefore, single top production provides a unique opportunity to study the  $Wtb$  structure and to measure  $V_{tb}$ . Experimental studies of this type are among the main goals of the single top physics. Using the single top quark search one can examine the effects of a deviation in the  $Wtb$  coupling from the SM structure and directly measure the CKM matrix element  $V_{tb}$ . Since the signal to background ratio is high after kinematical cuts applied the error of  $V_{tb}$  measurement as was shown in [8] is expected to be of order of 10% at the Tevatron RUN2. In the same time much higher statistics and good signal/background ratio at LHC allow considerably improve the measurement of  $V_{tb}$  value and test  $Wtb$  vertex. Since statistical error for  $10^5$  events is less than 1%, then uncertainty of  $Wtb$  vertex measurement at LHC depends mostly on the uncertainty of theoretical calculations for single top quark production cross section and for the backgrounds. That is why calculations of the next order corrections to the single top quark production including the corrections to the kinematical distributions but not only to the total events rate and a simulation of main backgrounds at the NLO level are important for the LHC.

Another important source of uncertainties in the  $Wtb$  vertex measurement comes from parton distribution uncertainty as well as from the accuracy of top-quark measurement. In case of Tevatron these uncertainties have been included into consideration [8]. However in case of LHC this point is not very clear since one does not know how large those uncertainties would remain when the experiment will start, and the parton distribution functions and the top mass will be measured in separate experiments. That is why at present stage we did not include the pointed uncertainties for the case of LHC.

### III. CONCLUSIONS

The study of the single top-quark production versus complete background processes has been done. For calculations a special generator has been created based on the CompHEP and PYTHIA/JETSET programs. The computation shows the importance of the QCD fake background which was not taken into account in the previous papers. Study of the effects of the initial and final state radiation for  $jbb$  process shows that such an approximative method of simulation of higher jet multiplicity process has the accuracy of order 10% or less for the rate and gives significantly softer  $p_T$  distribution of the radiating jet comparing to the complete calculations.

It was shown that after optimized cuts applied the signal from the single top quark can be extracted from the background with the signal to background ratio about 0.4 for the upgraded Tevatron and 1 for the LHC. The remaining after cuts single top rate in the *lepton + jets* mode is expected to be about 120 events at the upgraded Tevatron and about  $1.6 \cdot 10^5$  events at the low luminosity LHC operation with  $30 \text{ fb}^{-1}$  accumulated data and assumptions made above. One can expect that  $V_{tb}$  CKM matrix element can be measured at upgraded Tevatron with an accuracy about 10% and hopefully with an accuracy of the order of few % at LHC.

### Acknowledgments

Authors are grateful to members of the single top group of the D0 collaboration for useful discussions.

A. B. is grateful to S. F. Novaes for fruitful discussions, thank the Instituto de Física Teórica for its kind hospitality and acknowledges support from Fundação de Amparo à Pesquisa do Estado de São Paulo (FAPESP).

E. B. would like to thank H. Anlauf, P. Manakos, T. Ohl, A. Pukhov, V. Savrin, J. Smith, C.-P. Yuan, and B.-L. Young for discussions of different aspects of calculations used, he wishes to acknowledge the KEK Minami-Tateya (GRACE) collaboration for the kind hospitality during his visit at KEK and his colleagues from the CompHEP group for the interest and support.

E. B. and L. D. acknowledge the financial support of the Russian Foundation of Basic Research (grant No 96-02-19773a), the Russian Ministry of Science and Technologies, and the Sankt-Petersburg Grant Center.

- [1] F. Abe *et al.*, (CDF Collaboration), Phys. Rev. Lett. **74**, 2626 (1995)  
S. Abachi *et al.*, (DØ Collaboration), Phys. Rev. Lett. **74**, 2632 (1995);
- [2] Dicus and S. Willenbrock , Phys. Rev. D **34**, 155 (1986)  
C.-P. Yuan, Phys. Rev. D **41**, 42 (1990)  
G.V. Jikia and S.R. Slabospitsky, Phys. Lett **B295**, 136 (1992)  
R.K. Ellis and S. Parke, Phys. Rev. D **46**, 3785 (1992)  
G. Bordes and B. van Eijk, Z. Phys. **C57**, 81 (1993)  
D.O. Carlson and C.-P. Yuan, Phys. Lett. **B306**, 386 (1993)  
G. Bordes and B. van Eijk, Nucl. Phys. **B435**, 23 (1995)  
S. Cortese and R. Petronzio, Phys. Lett. **B253**, 494 (1991)  
D.O. Carlson, E. Malkawi and C.-P. Yuan, Phys. Lett. **B337**, 145 (1994)  
T. Stelzer and S. Willenbrock, Phys. Lett. **B357**, 125 (1995)  
R. Pittau, Phys. Lett. **B386**, 397 (1996)  
M. Smith and S. Willenbrock, Phys. Rev. D **54**, 6696 (1996)  
D. Atwood, S. Bar-Shalom, G. Eilam and A. Soni, Phys. Rev. D **54**, 5412 (1996), D. Atwood, S. Bar-Shalom, and A. Soni, Phys. Rev. D **57**, 2957 (1998)  
C.S. Li, R.J. Oakes and J.M. Yang, Phys.Rev. D**55**, 1672 (1997)  
C.S. Li, R.J. Oakes and J.M. Yang, Phys.Rev. D**55**, 5780 (1997)  
G. Mahlon, S. Parke, Phys.Rev. D**55**, 7249 (1997)  
A.P. Heinson, A.S. Belyaev, E.E. Boos, Phys. Rev. D**56**, 3114 (1997)  
T. Stelzer, Z. Sullivan, S. Willenbrock, Phys. Rev. D**56**, 5919 (1997)  
T. Tait, C.-P. Yuan, in hep-ph/9710372
- [3] R.D. Peccei and X. Zhang, Nucl.Phys. **B337**, 269 (1990)  
R.D. Peccei, S. Peris and X. Zhang, Nucl.Phys.B**349** 305 (1991)
- [4] T. Sjöstrand, Comp.Phys.Comm. **82**, 74 (1994)
- [5] E..E.Boos *et al.*, hep-ph/9503280,SNUTP-94-116;  
P.Baikov *et al.*, in Proc. of the Xth Int. Workshop on High Energy Physics and Quantum Field Theory, QFTHEP-95, ed. by B.Levtchenko, and V.Savrin, (Moscow, 1995), p.101
- [6] V.A. Ilyin, D.N. Kovalenko, and A.E. Pukhov, Int. J. Mod. Phys. C**7**, 761 (1996)  
D.N. Kovalenko and A.E. Pukhov, Nucl. Instrum. and Methods A **389**, 299 (1997)
- [7] S.Kawabata, Comp.Phys.Comm. **41** (1996) 127;
- [8] A.P. Heinson, A.S. Belyaev, E.E. Boos, Phys. Rev. D**56**, 3114 (1997)
- [9] M. Smith and S. Willenbrock, Phys. Rev. D **54**, 6696 (1996)  
T. Stelzer, Z. Sullivan, S. Willenbrock, Phys. Rev. D**56**, 5919 (1997)
- [10] M. Dittmar and H. Dreiner, Phys.Rev. D **55**, 167 (1997).
- [11] S. Moretti, Phys. Rev. D**56**, 7427 (1997).
- [12] N.V. Dokholyan and G.V. Jikia, Phys. Lett. B**336**, 251 (1994)  
E. Boos *et al*, Z.Phys. C **70** 255 (1996)
- [13] E. Laenen, J. Smith, and W.L. van Neereven, Nucl. Phys. B**369**, 54 (1992); Phys. Lett.B **321**, 254 (1994)  
E.L. Bereger and H.Contopanagos, Phys. Lett.B **361**, 115 (1995); Phys. Rev. D **54** 3085 (1996)  
S .Catani, M Mangano, P. Nason, and L. Trentadue, Phys. Lett.B **378**, 329 (1996); Nucl. Phys.B **478**, 273 (1996)

- [14] A. Belyaev, E. Boos, L. Dudko, A. Pukhov “W + 2 Jets Production at Tevatron: Vecbos and CompHEP Comparison”, D0-NOTE-2784, (1995), unpublished; hep-ph/9511306
- [15] TeV-2000 Study Group (D. Amidei et al.), FERMILAB-PUB-96-082.
- [16] J. Ohnemus , Phys. Rev. D **44**, 3477 (1991)
- [17] T. Han and S. Willenbrock, Phys.Lett B**273**, 167 (1991)  
J.Ohnemus and W.J.Stirling, Phys.Rev. D**47**, 2722(1993)  
H. Baer, B. Baiely and J. Owens, Phys.Rev. D**47**, 2730 (1993)
- [18] D0 Collaboration (S. Abachi et al.), Phys. Rev. D**52**, 4877 (1995)

Number of events

